



71st Conference of the Italian Thermal Machines Engineering Association, ATI2016, 14-16  
September 2016, Turin, Italy

## Optimization of heliostat field in a thermal solar power plant with an unfired closed Joule-Brayton cycle

M.Amelio<sup>a</sup>, P.Beraldi<sup>a</sup>, V. Ferraro<sup>a</sup>, M. Scornaienchi<sup>a</sup>, \*F.Rovense<sup>a</sup>

<sup>a</sup>DIMEG, University of Calabria, via Pietro Bucci, Arcavacata di Rende (Cs) 87036, Italy

### Abstract

In the last decades, concentrating solar power (CSP) has been gaining increasing attention as a sustainable technology for producing electricity. Nowadays, in the world, 483.6 MWs are produced by CSP plants of which 457 MW are already in commercial stage, whereas the other 430 MWs are under construction. In this paper, a solar tower with an unfired closed Joule-Brayton cycle of 10 MW peak power, located in Seville, is analyzed. The cycle, that employs only atmospheric air, without fuel consumption, relies on the possibility to vary the mean density of the air flowing in the plant. By using an auxiliary compressor and a bleed valve, a variable mass flow rate can be obtained so to keep the temperature at turbine inlet constant. On the other hand, in the concentrated solar plant, the number of installed heliostats can reflect towards the receiver the nominal thermal power, even with reduced values of the DNI. With the increase of the radiation, when the thermal energy flux achieves the limit tolerable by the receiver, a part of heliostats is defocused. On the contrary, in the presence of transients, due, for example, to clouds or in case of low solar radiation, the mirrors will be all, or in part, oriented towards the receiver face, so to keep constant the receiver outlet air temperature at the design value. Both the above mentioned control systems, without any fuel addition, act with the common goal of maintaining constant the air temperature at turbine inlet. However, they intervene at different times: at rated power, heliostats work, while the air flow rate is kept constant at the maximum value; when the nominal conditions are no longer achievable (the DNI values are insufficient), the adjustment is performed through the modulation of the pressure base control system, focusing the entire surface of the mirrors on the receiver. The analysis shows how the interaction between these systems influences the number and size of heliostats to be installed in the solar field. The study of the state of art has demonstrated that, in tower systems currently in operation, without storage, a solar multiple of 1.3 is generally used; our contribution shows how, with the air density control system, this value may be reduced, with consequent benefit on the heliostats cost. The numerical tests have been carried out by using the WINDELSOL software to optimize the heliostat field configuration and the THERMOFLOW, for the thermodynamic analysis.

© 2016 The Authors. Published by Elsevier Ltd. This is an open access article under the CC BY-NC-ND license (<http://creativecommons.org/licenses/by-nc-nd/4.0/>).

Peer-review under responsibility of the Scientific Committee of ATI 2016.

**Keywords:** concentrating solar power, solar-gasturbine, optimization of heliostat field, solar tower plant, control system

Corresponding author: Francesco Rovense  
E-mail address: [francesco.rovense@unical.it](mailto:francesco.rovense@unical.it)

## 1. Introduction

The use of solar energy as a source of energy production has reached a technological maturity such as to enable its adoption not only for the direct production of electricity, but also for the indirect production of energy carriers, like hydrogen [1][19]. Nowadays, the adoption of concentrating solar power (CSP) plants is spreading more and more. About 483.6 MWs of energy are produced by CSP plants: 457 MWs are generated by commercial towers, whereas 430 MWs are expected to be produced in a near future. [2]. In this paper, we propose a solar thermal power plant, that uses an air unfired Joule-Brayton cycle in closed loop. Nowadays, some examples of this kind of energy systems, in Europe, can be found in Spain [3] or in France [4].

The considered system, (shown in figure 1), is composed by a solar tower and heliostats field, an intercooler and regenerated gas turbine, a low temperature heat exchanger, an auxiliary compressor and a bleed valve. No combustor is used, though typically employed in this kind of plant [3,4], and the only thermal energy source is represented by the direct solar radiation.

The analysis proposed in this paper is aimed at determining the best configuration of the heliostats field, the solar multiple, and the tower, for the specific control system, so to minimize the LCOE.

### Nomenclature

GT	Gas turbine
DNI	Direct normal radiation [ $\text{W}/\text{m}^2$ ]
TIT	Temperature inlet turbine [ $^{\circ}\text{C}$ ] = $T_3$
SM	Solar multiple
$P_{1 \min}$	Minimum level of pressure base [bar]
$P_{1 \max}$	Maximum level of pressure base [bar]
LCoE	Levelized cost of electricity [ $\$/\text{kWh}$ ]
CSP	Concentrated solar power
$\beta$	Compressor/expansion ratio
$T_1$	Cycle base temperature [ $^{\circ}\text{C}$ ]
TOT	Temperature outlet turbine [ $^{\circ}\text{C}$ ] = $T_4$
$\Delta M_c$	Mass variation in the cycle [kg]
$\Delta \rho_c$	Density variation in the cycle [ $\text{kg}/\text{m}^3$ ]
$V_c$	Air volume of the system [ $\text{m}^3$ ]
$\Delta P_c$	Pressure base variation [bar]
R	Universal constant gas [ $\text{J}/\text{kgK}$ ]
$T_c$	Average temperature of cycle [ $^{\circ}\text{C}$ ]
$W_s$	Specific work [ $\text{kJ}/\text{kg}$ ]
$W_t$	Turbine work [ $\text{kJ}/\text{kg}$ ]
$W_{c1}$	Compressor work of first compressor [ $\text{kJ}/\text{kg}$ ]
$W_{c2}$	Compressor work of second compressor [ $\text{kJ}/\text{kg}$ ]
$c_p$	Heat capacity [ $\text{kJ}/\text{kg}^{\circ}\text{C}$ ]
$T_2$	Temperature outlet second compressor [ $^{\circ}\text{C}$ ]
$P_{\text{th SF}}$	Thermal power solar inlet solar field [ $\text{kW}_{\text{th}}$ ]
$\dot{m}$	Mass flow of the cycle [ $\text{kg}/\text{sec}$ ]
$\Delta H$	Enthalpy variation of the air between second compressor stage point and inlet turbine point [ $\text{kJ}/\text{kg}$ ]
$\alpha$	Pay back factor
$i$	Real discount rate
$n$	Useful life of plant [Years]
$k_{\text{ins}}$	Annual rate of insurance
$C_{\text{inv}}$	Investment cost [ $\$$ ]
$C_{\text{O\&M}}$	Operating and maintenance cost [ $\$$ ]
$E_{\text{net}}$	Net energy product [GWh]

1.1. Plant description

We consider a plant with an unfired intercooled and regenerated closed air Joule-Brayton from the nominal power of 10 MW. Figure 1 shows the system layout, whereas Table 1 summarizes the main plant characteristics of the plant.

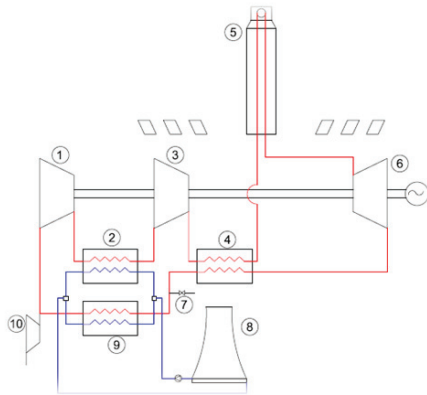


Fig. 1. Complete plant.

$\beta$	6
Peak mass flow	278 kg/s
$P_1$ min	1.01 bar
$P_1$ max	5.05 bar
$P_3$ max	30.3 bar
TIT	800 °C
$T_1$	35 °C
$\Delta H$	693.4 kJ/kg

Table 1. GT data performed in Thermoflex

The red line in the Figure 1 represents the path of the fluid work, whereas the blue line indicates the cycle made by the water in the cooling system. The air, after being compressed in the first compressor (1), passes into the intercooler (2), where it is cooled at the initial cycle condition. Subsequently it is recompressed by the second compressor (3), and it is sent to the first regenerator (4) and finally to the tower (5). Internally in the receiver of the tower, the air mass flow is heated up to a temperature of 800 °C. This value also represents the TIT of the GT, not making use of the fuel inside the cycle, and it is a compromise adding the CSP plant with the engine system [5]. The fluid at high enthalpy value expands in turbine (6) and is cooled in a heat exchanger (9) that cools the air mass flow, in order to reestablish the initial cycle conditions. After the cooling, the air is compressed again, and the cycle re-begins.

The system is able to vary the mass flow evolving in the cycle, while maintaining at a constant rate the volumetric flow system. This condition can be accomplished through the variation of pressure, operated by an auxiliary compressor (10), placed at GT intake, and by a vent valve (7), placed before the heat exchanger (9). In presence of high DNI values, the auxiliary compressor sucks air from the atmosphere, adding mass air in the cycle; vice versa, in presence of transients due to clouds or for low DNI values, the vent valve bleeds air to the ambient. The density air control implemented by these auxiliary components is necessary to adjust the exit air temperature from the receiver.

In this discussion, it was hypothesized that the TIT coincides with the outlet air temperature from the receiver, and there are no heat losses between the turbine and the receiver.

The choice of low TIT, does not require the cooling of the vanes of the turbine, thus favoring an increasing of net efficiency. The maximum and minimum temperatures ( $T_1$  e  $T_3$ ) are constant as well as the pressure ratio ( $\beta$ ) of the cycle and the plant volume in which evolves the working fluid. Is therefore possible to operate a change of the fluid density, through the only pressure base variation of the cycle.

The consequence is a mass variation inside the plant volume, according to the equation:

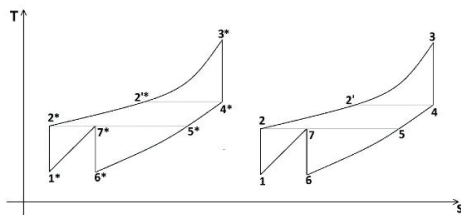


Fig. 2. T-s cycle diagram transformation

$$\Delta M_c = \Delta \rho_c V_c = \frac{\Delta p_c}{RT_c} V_c \quad (1)$$

In Figure 2, it is possible to observed the T-s diagram that translate from the 1-2-2'-3-4-5-6-7 cycle to the 1\*-2\*-2'\*-3\*-4\*-5\*-6\*-7\* cycle, when is performed the mentioned pressure base control. In this particular case an exaggerate increase of pressure has been operate to understand the make simpler the reading of the graph. In this way it is possible to maintain unaltered the thermodynamic cycle, and, thus, the extremes temperature of the cycle.

## 2. Methodology

In our analysis, we have chosen a 10MW plant size with a compression ratio ( $\beta$ ) of 6. The choice of having a low compression ratio in addition to the degree of heat recovery to be obtained through regeneration, depends upon the maximum pressure to which the receivers currently on the market may operate [6].

The SM is proper parameters in order to optimize the heliostat field and to determine the GT energy required and estimated the energy annual production [9].

The SM has been defined as the ratio between the thermal power of the heliostat surface and the rate electric power system [7].

$$SM = \frac{P_{th,SF}}{P_{rate,GT}} \quad (3)$$

The typical value of the SM is between 1.3 and 1.4 for plant without storage system, while it can also reach values that are 2.0 or higher in systems with thermal energy storage systems [8].

The configuration chosen for heliostats field is north field. In addition to the plant size [11], this choice is also justified by the difficulty deriving from the use of a surround field setup to control the density variation within the receiver [10]. The passage of clouds in a part of the field would create a decrease of the thermal power in input to the receiver, and thus a change of the temperature inside the air receiver, that would be difficult to control with the control system analyzed.

Equation 4 [11] to estimate the tower height has been used.

$$H_t = 29.1 + 0.5113 * P_{th,SF} - 0.00887 * P_{th,SF}^{1.5} + 32801.719 * P_{th,SF}^{-2} \quad (4)$$

The thermal power in input to the receiver has been evaluated as the entire heat input power to the Brayton cycle and calculated by the equation (5) through the data analyzed in Thermoflex (Table 1).

$$P_{th,SF} = \dot{m} \times \Delta H \quad (5)$$

By using the software WinDelsol, the best configuration for the heliostats field, the optical matrix, the optical losses of the field and the thermal receiver have been calculated. Then the data obtained by WinDelsol code with CSP system, simulated in Thermoflex software, have been interconnected. Thermoflex was used to simulate the yearly plant, hypothesized located in Seville. The data using in this analysis, to simulate an operating year of this plant, in term of DNI, azimuth angle, zenith angle, ambient temperature, and relative humidity from TMY3[12] of this town have been extrapolated. To explain the performance of the system, a case of a particular day,(21 June) have been shown.

Finally, to compare the result of the plant with density control system and heliostat control system in optimum configuration, a plant in hybrid configuration have been assumed. This last one has a GT with the same peak power level as well as the TIT but not use the density control system, operating at atmospherical pressure condition. To control the cloud transient, in fact, the employment of a combustor using methane gas ( $CH_4$ ) to maintain the TIT at constant value of 800°C have been hypothesize. The analysis for CSP plant, are the same of the density control system in term of SM, and the results of the hybrid configuration plant are contained in [20].

## 3. Simulation

This section is devoted to the presentation of the plant operation conditions with the aim of highlighting the behavior of the two control systems. In addition, we shall show the results of the simulations with the WinDelsol software for different system configurations, and we shall describe the LCoE method used.

### 3.1. Solar field control system analysis

We consider the behavior of the heliostat field during a day without extreme variation of the DNI. The design point of CSP plant is  $850 \text{ W/m}^2$ ; so for higher level of this value, performs the heliostat control system that defocused a percentage of reflective area. Table 2 and Figure 3 show the result obtained by ThermoFlex; it is possible to observe how the control system of the heliostat field perform, i.e. through the defocusing of a determined number of heliostats when the direct solar radiation is too high compared to the design point. In Figures 3 and 4 and it is possible to observe that for  $SM=1$  no defocusing of the heliostats is performed.

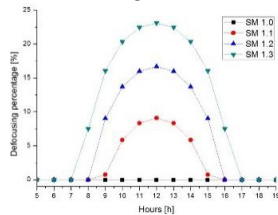


Fig. 3. Defocusing percentage of the heliostat field vs hour day

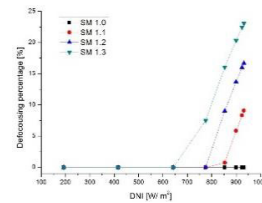


Fig. 4. Defocusing percentage of the heliostat field vs DNI

By increasing, the SM and, thus, the number of available heliostats, it is necessary to defocus more heliostats in the central hours of the day with high DNI values.

Figure 3 shows the trend of heliostat defocusing during this day (June 21st) with a DNI peak of  $932 \text{ W/m}^2$ . In Figure 4, the performance of the heliostat control system vs direct normal radiation for the same day is shown. In both cases, it is possible to note as the adjustment of the heliostats is activated, when the DNI design point is achieved, especially in the middle hours of the day. On the contrary, it is possible to note that the adjustment of the heliostats is not necessary for low DNI values, and, thus, in the early hours of the morning and the last afternoon. In these moments, the entire heliostat field on the receiver is focused, so to provide the maximum value of thermal energy, and no adjustment is possible.

### 3.2. Density control system analysis

The density control system, by varying the pressure base of the cycle, produces as useful effect the translation of the thermodynamic cycle, in the T-s diagram, as the DNI varies, but keeping fixed the characteristic temperatures.

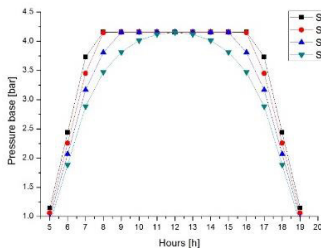


Fig. 5. Pressure base adjustment in time function for different SM

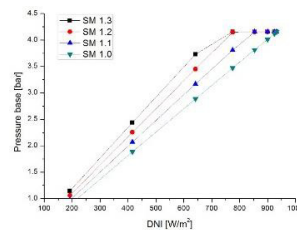


Fig. 6. Pressure base adjustment in DNI function for different SM

From Figure 6, it is possible to note, for considered day, the maximum value of pressure adjustment, that is 4.15 bar whereas the minimum value is set to 1.01 bar. Figure 5 shows the trend of the pressure base control versus DNI.

### 3.3. Solar field simulation

In this section, we report the heliostats field simulation performed by the WinDelsol software for three values of the SM. The next Figures report the optical field losses [11] and the receiver losses for each configuration. More specifically, Figures a) report the heliostats field losses, as blocking, atmospheric transmissivity, spillage, and total optical efficiency, whereas Figures b) show the map incident heat flux on the receiver.

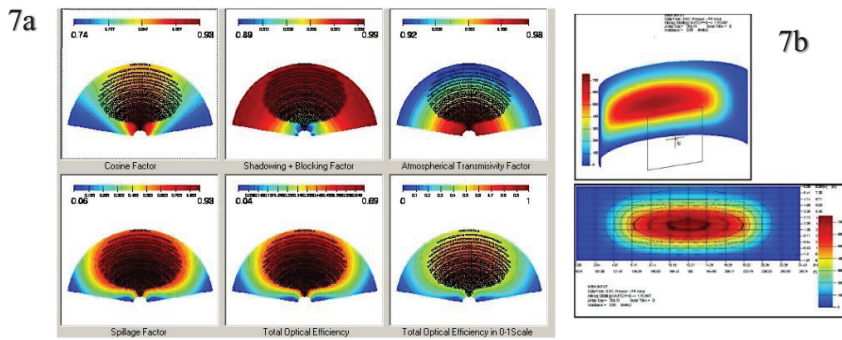


Fig. 7.a and 7.b show the configuration for SM = 1.3 of the heliostats field. Fig. 7.a) solar field configuration for SM of 1.3 Fig. 7.b) map incident flux on receiver surface

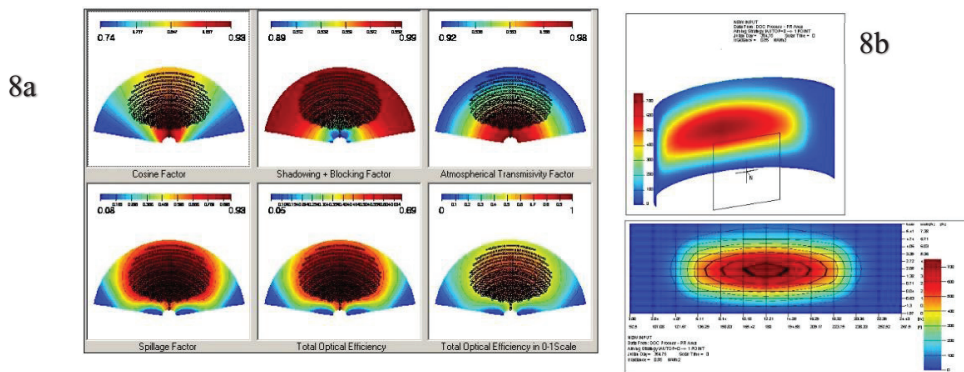


Fig. 8. a) Solar field configuration for SM of 1.2. Fig. b) map incident flux on receiver surface

Figures 8.a and 8.b show the results for the configuration for the SM=1.2, while Figures 9.a and 9.b show the analysis for the SM=1.1. Finally, Figures 10.a and 10.b shows the results for the SM= 1.0.

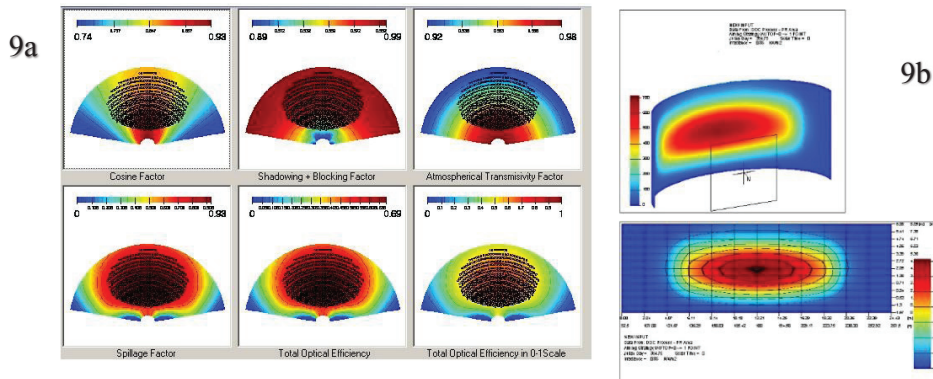


Fig. 9.a) Solar field configuration for SM of 1.1, Fig. 9b) map incident flux on receiver surface

The results obtained by WinDelsol software as input data in Thermoflex software have been used. In particular, the loss coefficients show in figure 7a, 8a, 9a, 10a, for each SM configuration, and the data listed in the table 2 have been inserted.



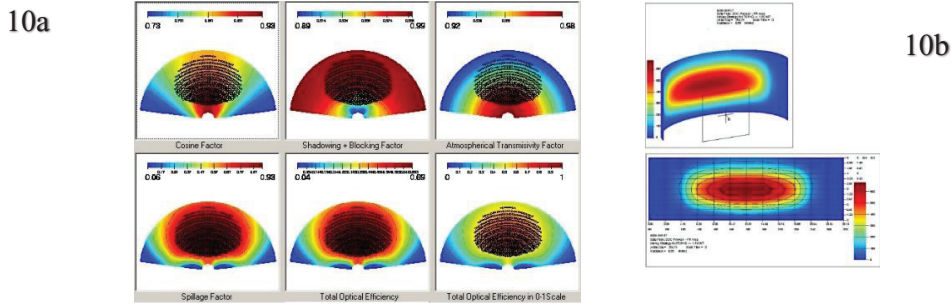


Fig. 10 a) Solar field configuration for SM of 1. Fig 10 b) map incident flux on receiver surface

Table 2. Data CSP plants using in Thermoflex simulation

SM	1	1.1	1.2	1.3
Heliostat number	410	451	492	533
Tower structure height [m]	31,17	32,69	34,14	35,53
Total reflective area [m <sup>2</sup> ]	49268	54195	59122	64049
Inner radius [m]	23,37	24,52	25,61	26,65
Outer radius [m]	218,20	228,8	239,00	247,20

3.4. Cost analysis

In order to perform the economic analysis, we have used the economic indicator LCOE expressed in USD / kW<sub>hel</sub>. Since the calculation of the LCOE depends on many different factors, with the aim of making the proposed analysis easily reproducible, some simplifications have been carried out [8]. The relation of the LCOE (6) used in this work is [13].For the costs and financial data we referred to [14], [15] [16].

$$LCOE = \frac{\alpha * C_{inv} + C_{fuel} + C_{O\&M}}{E_{Net}} \quad (6)$$

4. Calculation

The aim of the economic evaluation is the minimization of the LCOE by the optimal sizing of the solar field. In order to perform the analysis, we have used the financial data in Table 4, taken from [17]. Figure 11 shows the LCOE analysis.

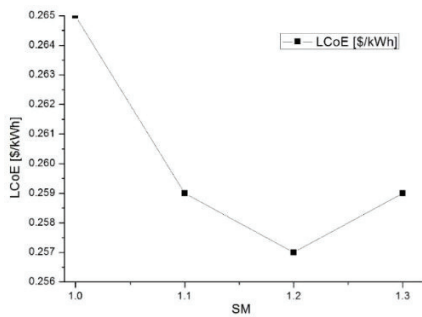


Fig. 11. LCOE trend vs SM

Table 3. Investment cost, energy production and LCOE for each SM

SM	1	1.1	1.2	1.3
Cinv [MUSD]	50.40	54.01	57.60	61.17
Enet [MWh]	21.40	23.30	24.85	26.02
LCOE [USD/kWh]	0.265	0.259	0.257	0.259

Table 4. Total operation hours and its percentage of density control system

SM	1	1.1	1.2	1.3
Tot [h]	2977	2551	2114	1784
Density control system [%]	97.5	82.2	67.1	55.8

The economic analysis and the value of the LCOE has been determined as a function of the solar multiple. It is possible to observed in Figure 11, that the optimum value is obtained for a solar multiple of 1.2 and is equal to 0.257 \$/ KWh. Thus, the LCOE value, computed in this analysis, is less than 1.3 and 1.4, that represent the typical values for the CSP plants. As it is possible to note by increasing the SM, the adjustment is operated by the heliostat's control system, whereas for low value of the SM, the adjustment is performed by the mass flow control system. In particular, for the SM=1 the mass flow regulation system works almost exclusively whereas for the SM=1.3 the two adjustment systems work both for about 50% of the operation hours.

## 5. Conclusion

We have observed that by the two control systems it is possible to increase the annual energy production minimizing the LCOE. In particular, by increasing the SM through the mirror field adjustment is possible to produce electricity at nominal operating conditions at full power for more hours during the year, whereas the mass flow control system is able to produce energy when the DNI have a low value.

The optimum solar multiple value is 1.2, with a minimum value of LCOE of 0.257 \$/kWh. The result is very promising, and it is very similar at the values of the other CSP system [18]. A lower value of the SM has a direct impact on the plant costs, contributing to reduce them. By considering that, in our analysis, the 25% of the system costs is related to the heliostats field, the estimated cost reduction is around 3.57 M \$. Finally, this kind of plant, with other one of same GT peak power but in hybrid configuration to compare the result have been assumed [20]. Like the result, comparing the density control system plant with those the hybrid plant, we have that 266 g of CO<sub>2</sub> per kWh product have been avoided.

## References

- [1] Nastasi B. Renewable hydrogen potential for low-carbon retrofit of the building stocks. *Energy Procedia* 82 (2015) 944 – 949
- [2] <http://www.cspworld.org/cspworldmap>
- [3] M. Quero, R.Korzynietz, M. Ebert, AA. Jiménez,A. del Río, JA. Brioso. Solugas - Operation experience of the first solar hybrid gas turbine system at MW scale.
- [4] B. Grangea, C. Daleta, Q. Falcoza, F. Siroso, A.Ferrièrea, (2014) , Simulation of a Hybrid Solar Gasturbine Cycle with Storage Integration, SolarPACES 2013 International Conference.
- [5] W.B. Stine, M. Geyer, "Power Cycles for Electricity Generation" in *Power from the sun*, 2001
- [6] P. Poživila, V. Agab, A. Zagorskiyb, A. Steinfelda. A pressurized air receiver for solar-driven gas turbines- *Energy Procedia* 49 ( 2014 ) 498 – 503 SolarPACES 2013 International Conference
- [7] Maroni & Partners-"Impianti solari termodinamici: stato dell'arte e incentivazione"-ANEST (Associazione Nazionale Energia Solare Termodinamica), 2014
- [8] Irena (International Renewable Energy Agency)-"Renewable energy technologies: cost analysis series"-Volume 1: Power Sector-Concentrating Solar Power"-June, 2012
- [9] Solar Thermal Power Plants: Achievements and Lessons Learned Exemplified by the SSPS Project in Almeria/Spain. Federico G. Casal. Springer Science & Business Media, 06 December 2012
- [10] V. Casamassima, G. Antonio Guagliardi-"Modello matematico di un impianto solare a concentrazione ibrido con turbina a gas e simulazione di transitori normali e di emergenza"- RSE (Ricerca Sistema Energetico), Gennaio 2013
- [11] William B. Stine, Michael Geyer -"Power from the sun"- 2001 <http://www.powerfromthesun.net/book.html>
- [12] S. Wilcox and W. Marion. (2008, May). User's Manual for TMY3 Data Sets. National Renewable Energy Laboratory. City, State or Country. [NREL/TP-581-43156]. <http://www.nrel.gov/>
- [13] J. Spelling, B. Laumert, T. Fransoon-"Advanced hybrid solar tower combined-cycle power plants"-*Energy Procedia*, SolarPACES 2013
- [14] Craig S. Turchi, Garivin A. Heath-"Molten salt power tower cost model for the system advisor model (SAM)"-NREL (National Renewable Energy Laboratory), Febbraio 2013
- [15] Gregory J. Kolb, Clifford K. Ho, Thomas R. Mancini, Jesse A. Gary-"Power tower technology roadmap and cost reduction plan"-Sandia report, Aprile 2011
- [16] THERMOFLOW package, "THERMOFLEX" Fully-Flexible Heat Balance Engineering Software
- [17] R.Pitz-Pall, J. Dersch, B. Milow-"European concentrated solar thermal road-mapping"-report ECOSTAR, 2003
- [18] International Renewable Energy Agency, "RENEWABLE ENERGY TECHNOLOGIES: COST ANALYSIS SERIES" Volume 1: Power Sector Issue 2/5 Concentrating Solar Power June 2012
- [19] Nastasi B, Lo Basso G. Hydrogen to link heat and electricity in the transition towards future Smart Energy Systems. *Energy* 2016. In press.
- [20] N.Gallicchio. Interazione fra la regolazione degli eliostati e quella della turbina a gas, in un impianto solare termodinamico. Department of mechanical energy and management engineer. UNICAL. Master thesis. M.Amelio, F.Rovense. December 2015